

## Jahnsite, $\text{CaMn}^{2+}\text{Mg}_2(\text{H}_2\text{O})_8\text{Fe}^{3+}_2(\text{OH})_2[\text{PO}_4]_4$ : A Novel Stereoisomerism of Ligands about Octahedral Corner-Chains

PAUL BRIAN MOORE, AND TAKAHARU ARAKI

Department of the Geophysical Sciences, The University of Chicago,  
Chicago, Illinois 60637

### Abstract

Jahnsite,  $\text{CaMn}^{2+}\text{Mg}_2(\text{H}_2\text{O})_8\text{Fe}^{3+}_2(\text{OH})_2[\text{PO}_4]_4$ ,  $a$  14.94(2) Å,  $b$  7.14(1) Å,  $c$  9.93(1) Å,  $\beta$  110.16(8)°,  $P2/a$ ,  $Z = 2$ , is one of the 7 Å octahedral corner-linked chain structures allied to laueite, pseudolaueite, childrenite, etc.  $R(hkl) = 0.09$  for 2292 independent non-zero reflections.

The structure is based on a backbone of corner-linked ...  $\text{Fe}^{3+}\text{-OH-Fe}^{3+}$  ... octahedra with a novel arrangement of  $[\text{PO}_4]$  tetrahedra about these chains. The structure possesses dense slabs of  $[\text{CaMn}^{2+}\text{Fe}^{3+}_2(\text{OH})_2[\text{PO}_4]_4]^{+}$  oriented parallel to  $\{001\}$  which are bridged by  $\text{PO}_4$  corner-sharing to  $\text{Mg}(\text{O},\text{H}_2\text{O})_8$  octahedra.

Polyhedral interatomic averages are  ${}^{\text{v}}\text{Fe}(1)\text{-O}$  1.973 Å,  ${}^{\text{v}}\text{Fe}(2)\text{-O}$  1.973,  ${}^{\text{v}}\text{Ca-O}$  2.418,  ${}^{\text{v}}\text{Mn}^{2+}\text{-O}$  2.190,  ${}^{\text{v}}\text{Mg}(1)\text{-O}$  2.088,  ${}^{\text{v}}\text{Mg}(2)\text{-O}$  2.089,  ${}^{\text{v}}\text{P}(1)\text{-O}$  1.543, and  ${}^{\text{v}}\text{P}(2)\text{-O}$  1.533.

### Introduction

Jahnsite is one of several new mineral species described by Moore (1974) which occur as late-stage hydrothermal products of the decomposition of triphylite-lithiophilite in pegmatites. A rather frequently found mineral, it occurs in a paragenesis with laueite, strunzite, and stewartite, suggesting that these minerals have a closely-related structural principle. The jahnsite structure type provides a range of compositions from an aluminum analogue  $\text{Ca}(\text{Fe},\text{Mn})^{2+}\text{Mg}_2(\text{H}_2\text{O})_8\text{Al}^{3+}_2(\text{OH})_2[\text{PO}_4]_4$  to highly oxidized large-cation deficient material  $(\text{Ca},\text{Mn}^{2+})_{-1}(\text{Fe}^{3+},\text{Mg})_{-2}(\text{OH},\text{H}_2\text{O})_8\text{Fe}^{3+}_2(\text{OH})_2[\text{PO}_4]_4$ . A closely related structure apparently occurs in segelerite,  $\text{CaMg}(\text{H}_2\text{O})_4\text{Fe}^{3+}(\text{OH})[\text{PO}_4]_2$  (Moore, 1974).

Our laboratory has been much interested in the systematics of transition-metal phosphate structures, especially with respect to polynuclear clustering of the transition metals and with problems of ligand stereoisomerisms about these clusters. Additionally, we seriously doubt if, without a detailed structure analysis, sensible formulae can be applied to these complex structures wherein the role of  $(\text{H}_2\text{O})$  is often manifold.

### Experimental

The crystal cell parameters for jahnsite are  $a$  14.94(2) Å,  $b$  7.14(1) Å,  $c$  9.93(1) Å,  $\beta$  110.16(8)°,  $Z = 2$ , with formula unit  $\text{CaMn}^{2+}\text{Mg}_2(\text{H}_2\text{O})_8\text{Fe}^{3+}_2(\text{OH})_2[\text{PO}_4]_4$  derived from the study of Moore

(1974). Weak  $0k0$  reflections with  $k \neq 2n$  and the systematic absence  $h = 2n$  for  $h0l$  established the space group as  $P2/a$  or  $Pa$ . The centric group,  $P2/a$ , was chosen on the basis of the observed morphological holosymmetry.

A suitable single crystal nearly equant in shape and 0.2 mm in mean dimension was selected from the type specimen collected by P.B.M. at the Tip Top pegmatite, near Custer, South Dakota.

With  $[010]$  as the rotation axis, reflections to  $2\theta = 65^\circ$  were gathered on a PAILRED diffractometer utilizing a graphite monochromator and  $\text{MoK}\alpha$  radiation. Twenty-second background counts were taken on each side of the peak. The scan rate was  $2.5^\circ/\text{minute}$  with half-scan interval of  $2.0^\circ$ , widening to  $2.8^\circ$  at high levels.  $\omega$ -scans revealed low absorption anisotropy, so a correction was not applied. Symmetry-equivalent reflections were averaged and the data were processed by conventional computational procedures to obtain  $|F(\text{obs})|$ .

### Solution and Refinement

A three-dimensional Patterson synthesis,  $P(uvw)$ , revealed strong concentrations of vectors at  $0, \frac{1}{2}, 0$ ;  $\frac{1}{2}, 0, 0$ ;  $\frac{1}{4}, 0, 0$ ;  $\frac{1}{4}, \frac{1}{2}, 0$  and immediately led to a model based on octahedral chains. Unfortunately, a pronounced substructure, discussed further on, led to ambiguities in the  $y$ -coordinates for the  $[\text{PO}_4]$  tetrahedra and the  $\text{Mg}(\text{O},\text{H}_2\text{O})_8$  octahedra.

Approximate location of the atoms in the dense

slabs parallel to {001} was achieved through the  $\beta$ - and  $\gamma$ '-syntheses of Ramachandran and Srinivasan (1970). Correct locations for the  $y$ -coordinates of the phosphorus and magnesium atoms were achieved through a careful inspection of the bond distances in the partly determined structure.

When all atoms were located, refinement of atomic coordinates and isotropic thermal vibration parameters proceeded from the scattering curves of Cromer and Mann (1968) for  $\text{Ca}^{1+}$ ,  $\text{Mn}^{2+}$ ,  $\text{Fe}^{2+}$ ,  $\text{Mg}^{1+}$ ,  $\text{P}^0$  and  $\text{O}^{1-}$ . The full-matrix refinement, on IBM-360 computer, and using a local, unpublished program modified from the ORFLS program of Busing, Martin, and Levy (1962) converged, for different structure factor magnitudes, to the values of  $R(hkl)$  given in Table 1. Table 2 provides the final atomic coordinates and isotropic thermal vibration parameters and Table 3 is the list of structure factors.

**Description of the Structure**

*General Structural Features and Principles*

Moore (1970a) outlined the general problems associated with the "7 Å octahedral corner-linked chain structures," which include a large number of discrete structure types. The dominating motif of these structures is an infinitely extending octahedral chain which involves  $\text{Me}^{3+}$  ( $=\text{Al}^{3+}, \text{Fe}^{3+}$ ) cations and opposing apical corner-links of  $(\text{OH})^-$  anions. This structural backbone is featured in Figure 1. We shall find it convenient to refer to a structural prototype, that is, the simplest arrangement which affords such a corner-linked chain. This is evidently the structure of  $\text{Fe}^{3+}(\text{OH})[\text{SO}_4]$  (and isostructural  $\text{In}^{3+}(\text{OH})[\text{SO}_4]$ ), described by Johansson (1962). It possesses the octahedral chains parallel to the  $a$ -axis which link laterally by  $[\text{SO}_4]$  tetrahedra to form an indefinitely extending network of octahedra and tetrahedra.

Baur (1969) has noted that, in the 7 Å chain

TABLE 1. Dependence of  $R(hkl)$  on  $|F(hkl)|$  for Jahnsite

$R(hkl) = \frac{\sum  F(\text{obs})  -  F(\text{calc}) }{\sum  F(\text{obs}) }$			
$F(hkl)$		Number	$R(hkl)$
Above 0.0		3234	0.12
" 6.0		2292	0.09
" 18.0		1207	0.06
" 36.0		415	0.05
" 61.0		147	0.04

TABLE 2. Jahnsite. Atomic Coordinates and Isotropic Thermal Vibration Parameters\*

Atom	x	y	z	B(Å <sup>2</sup> )
Fe(1)	0.0000	0.0000	0.0000	1.58(3)
Fe(2)	.0000	.5000	.0000	1.70(3)
Mg(1)	.5000	.0000	.5000	1.21(7)
Mg(2)	.2500	.4963(3)	.5000	0.96(7)
Ca	.2500	-.0249(3)	.0000	1.69(3)
Mn	.2500	.4775(2)	.0000	1.12(3)
P(1)	.1830(1)	.2615(2)	.1881(2)	.92(2)
O(1)	.2758(4)	.2345(7)	.1512(6)	1.83(6)
O(2)	.2041(4)	.2956(7)	.3462(6)	1.65(8)
O(3)	.1229(4)	.0827(7)	.1399(6)	1.57(8)
O(4)	.1369(3)	.4352(6)	.0941(5)	1.15(7)
F(2)	.0813(1)	.7476(2)	.7978(2)	.87(2)
O(5)	.1890(4)	.6984(7)	.8553(6)	1.52(8)
O(6)	.0497(3)	.7802(7)	.6381(5)	1.47(8)
O(7)	.0747(3)	.9293(6)	.8791(5)	1.29(7)
O(8)	.0245(3)	.5881(6)	.8314(5)	1.29(7)
OH	.0256(3)	.7509(6)	.0935(5)	1.06(6)
OW(1)	.2231(4)	.7185(8)	.3445(6)	2.09(9)
OW(2)	.4497(4)	.2130(8)	.3452(6)	2.37(9)
OW(3)	.6307(4)	-.0066(8)	.4629(6)	2.18(9)
OW(4)	.3917(4)	.5131(7)	.5115(5)	1.72(9)

\* Estimated standard errors refer to the last digit.

structures he investigated, the octahedral backbone is linked laterally by tetrahedra to similar backbones, forming dense slabs. Between these slabs are more weakly linked bridging groups, usually consisting of insular  $\text{Me}^{2+}(\text{O}, \text{H}_2\text{O})_6$  octahedra.

Moore (1970a) has singled out two kinds of isomerism which explain the unusual diversity of the 7 Å chain structures. The first kind involves the arrangements of the  $[\text{PO}_4]$  and  $(\text{H}_2\text{O})$  ligands about the backbone, of which seven types of isomerisms which permit the formation of slabs were discerned. In addition, the bridging  $\text{Me}^{2+}(\text{O}, \text{H}_2\text{O})_6$  octahedral species between the slabs can exhibit *cis* or *trans* stereoisomerism. Jahnsite and segelerite (based on a preliminary structure analysis) belong to arrangement VI (see Moore, 1970a) of tetrahedra about the backbone, an arrangement postulated on stereochemical grounds and heretofore unknown in mineral structures. The distinction between jahnsite and segelerite apparently occurs in the conformation of the bridging octahedral species and locations of the  $[\text{PO}_4]$  tetrahedra.

The idealized jahnsite slab (Fig. 2) is formed by the coupling of octahedral backbones by infinitely extending columns of  $\text{Me}^{2+}\text{O}_6$  edge-sharing octahedra. The large  $\text{Me}^{2+}$  cations, such as  $\text{Ca}^{2+}$  and  $\text{Mn}^{2+}$ , form six- to eight-fold coordinated polyhedra (see Fig. 3). In the ideal structure these polyhedra each share two edges with the  $\text{Me}^{3+}\text{O}_6$  octahedra at the same level, two edges with the  $[\text{PO}_4]^{3-}$



JAHNSITE, A NOVEL STEREOISOMERISM

TABLE 3, Continued

A	k	l	Fobs	Fcalc	A	k	l	Fobs	Fcalc	A	k	l	Fobs	Fcalc	A	k	l	Fobs	Fcalc	A	k	l	Fobs	Fcalc
12	2	-13	23.8	15.7																				
12	2	-14	7.3	4.2																				
12	2	-15	11.0	17.5																				
12	2	-16	11.5	10.3																				
12	2	-17	4.4	6.7																				
12	2	-18	8.1	6.0																				
12	2	-19	13.0	9.7																				
12	2	-20	17.5	8.0																				
12	2	-21	14.7	8.2																				
12	2	-22	9.2	4.8																				
12	2	-23	5.1	7.4																				
12	2	-24	26.3	11.1																				
12	2	-25	4.7	8.3																				
12	2	-26	4.1	6.4																				
12	2	-27	13.7	6.2																				
12	2	-28	11.4	5.1																				
12	2	-29	11.5	3.0																				
12	2	-30	4.7	2.5																				
12	2	-31	5.3	0.8																				
12	2	-32	6.9	1.0																				
12	2	-33	8.6	5.5																				
12	2	-34	6.4	6.2																				
12	2	-35	10.6	11.0																				
12	2	-36	7.4	6.7																				
12	2	-37	2.4	7.7																				
12	2	-38	4.7	3.1																				
12	2	-39	5.5	7.7																				
12	2	-40	4.1	6.7																				
12	2	-41	4.6	4.8																				
12	2	-42	6.2	3.5																				
12	2	-43	4.3	6.3																				
12	2	-44	4.8	8.3																				
12	2	-45	6.1	3.5																				
12	2	-46	13.2	6.5																				
12	2	-47	5.0	6.5																				
12	2	-48	5.2	4.5																				
12	2	-49	5.7	4.5																				
12	2	-50	11.7	13.6																				
12	2	-51	11.6	13.6																				
12	2	-52	13.5	12.9																				
12	2	-53	17.1	15.8																				
12	2	-54	15.2	14.5																				
12	2	-55	13.0	13.9																				
12	2	-56	25.0	18.0																				
12	2	-57	17.5	16.0																				
12	2	-58	4.4	6.6																				
12	2	-59	4.5	6.4																				
12	2	-60	4.6	4.1																				
12	2	-61	6.6	5.3																				
12	2	-62	4.6	3.2																				
12	2	-63	10.6	10.6																				
12	2	-64	4.4	6.1																				
12	2	-65	11.3	13.2																				
12	2	-66	5.0	6.5																				
12	2	-67	5.2	4.5																				
12	2	-68	5.7	4.5																				
12	2	-69	11.7	13.6																				
12	2	-70	11.6	13.6																				
12	2	-71	13.5	12.9																				
12	2	-72	17.1	15.8																				
12	2	-73	15.2	14.5																				
12	2	-74	13.0	13.9																				
12	2	-75	25.0	18.0																				
12	2	-76	17.5	16.0																				
12	2	-77	4.4	6.6																				
12	2	-78	4.5	6.4																				
12	2	-79	4.6	4.1																				
12	2	-80	6.6	5.3																				
12	2	-81	4.6	3.2																				
12	2	-82	10.6	10.6																				
12	2	-83	4.4	6.1																				
12	2	-84	11.3	13.2																				
12	2	-85	5.0	6.5																				
12	2	-86	5.2	4.5																				
12	2	-87	5.7	4.5																				
12	2	-88	11.7	13.6																				
12	2	-89	11.6	13.6																				
12	2	-90	13.5	12.9																				
12	2	-91	17.1	15.8																				
12	2	-92	15.2	14.5																				
12	2	-93	13.0	13.9																				
12	2	-94	25.0	18.0																				
12	2	-95	17.5	16.0																				
12	2	-96	4.4	6.6																				
12	2	-97	4.5	6.4																				
12	2	-98	4.6	4.1																				
12	2	-99	6.6	5.3																				
12	2	-100	4.6	3.2																				
12	2	-101	10.6	10.6																				
12	2	-102	4.4	6.1																				
12	2	-103	11.3	13.2																				
12	2	-104	5.0	6.5																				
12	2	-105	5.2	4.5																				
12	2	-106	5.7	4.5																				
12	2	-107	11.7	13.6																				
12	2	-108	11.6	13.6																				
12	2	-109	13.5	12.9																				
12	2	-110	17.1	15.8																				
12	2	-111	15.2	14.5																				
12	2	-112	13.0	13.9																				
12	2	-113	25.0	18.0																				
12	2	-114	17.5	16.0																				
12	2	-115	4.4	6.6																				
12	2	-116	4.5	6.4																				
12	2	-117	4.6	4.1																				
12	2	-118	6.6	5.3																				
12	2	-119	4.6	3.2																				
12	2	-120	10.6	10.6																				
12	2	-121	4.4	6.1																				
12	2	-122	11.3	13.2																				
12	2	-123	5.0	6.5																				
12	2	-124	5.2	4.5																				
12	2	-125	5.7	4.5																				
12	2	-126	11.7	13.6																				
12	2	-127	11.6	13.6																				
12	2	-128	13.5	12.9																				
12	2	-129	17.1	15.8																				
12	2	-130	15.2	14.5																				
12	2	-131	13.0	13.9																				
12	2	-132	25.0	18.0																				
12	2	-133	17.5	16.0																				
12	2	-134	4.4	6.6																				
12	2	-135	4.5	6.4																				
12	2	-136	4.6	4.1																				
12	2	-137	6.6	5.3																				
12	2	-138	4.6	3.2																				
12	2	-139	10.6	10.6																				
12	2	-140	4.4	6.1																				
12	2	-141	11.3	13.2																				
12	2	-142	5.0	6.5																				
12	2	-143	5.2	4.5																				
12	2	-144	5.7	4.5																				
12	2	-145	11.7	13.6																				
12	2	-146	11.6	13.6																				
12	2	-147	13.5	12.9																				
12	2	-148	17.1	15.8																				
12	2	-149	15.2	14.5																				
12	2	-150	13.0	13.9																				
12	2	-151	25.0	18.0																				
12	2	-152	17.5	16.0																				
12	2	-153	4.4	6.6																				
12	2	-154	4.5	6.4																				
12	2	-155	4.6	4.1																				
12	2	-156	6.6	5.3																				
12	2	-157	4.6	3.2																				
12	2	-158	10.6	10.6																				
12	2	-159	4.4	6.1																				
12	2	-160	11.3	13.2																				
12	2	-161	5.0	6.5																				
12	2	-162	5.2	4.5																				
12	2	-163	5.7	4.5																				
12	2	-164	11.7	13.6																				
12	2	-165	11.6	13.6																				
12	2	-166	13.5	12.9																				
12	2	-167	17.1	15.8																				
12	2	-168	15.2	14.5																				
12	2	-169	13.0	13.9																				
12	2	-170	25.0	18.0																				
12	2	-171	17.5	16.0																				
12	2	-172	4.4	6.6																				
12	2	-173	4.5	6.4																				
12	2	-174	4.6	4.1																				
12	2	-175	6.6	5.3																				
12	2	-176	4.6	3.2																				
12	2	-177	10.6	10.6																				
12	2	-178	4.4	6.1																				
12	2	-179	11.3	13.2																				
12	2	-180	5.0	6.5																				
12	2	-181	5.2	4.5																				
12	2	-182	5.7	4.5																				
12	2	-183	11.7	13.6																				
12	2	-184	11.6	13.6																				
12	2	-185	13.5	12.9																				
12	2	-186	17.1	15.8																				
12	2	-187	15.2	14.5																				
12	2	-188	13.0	13.9																				
12	2	-189	25.0	18.0																				
12	2	-190	17.5	16.0																				
12	2	-191	4.4	6.6																				
12	2	-192	4.5	6.4																				
12	2	-193	4.6	4.1																				
12	2	-194	6.6	5.3																				
12	2	-195	4.6	3.2																				
12	2	-196	10.6	10.6																				
12	2	-197	4.4	6.1																				
12	2	-198	11.3	13.2																				
12	2	-199	5.0	6.5																				
12	2	-200	5.2	4.5																				

TABLE 3, Continued

Table with 21 columns: A, K, I, Fobs, Fcalc, A, K, I, Fobs, Fcalc, A, K, I, Fobs, Fcalc, A, K, I, Fobs, Fcalc, A, K, I, Fobs, Fcalc. The table contains numerical data for various experimental runs, including observations (Fobs) and calculations (Fcalc) for different parameters (A, K, I).





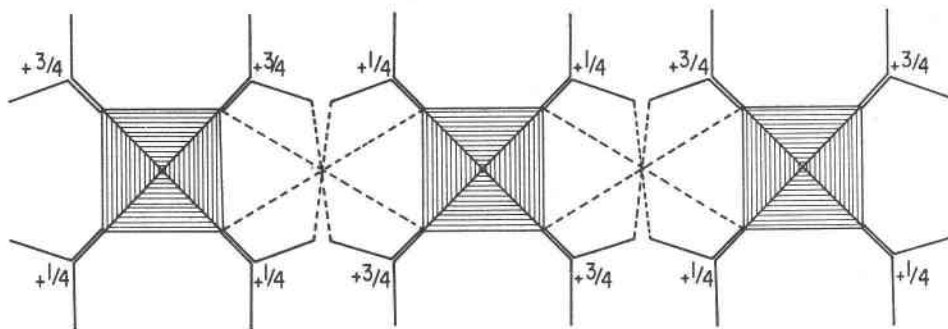


FIG. 2. Idealization of the slab with composition  $[\text{Me}^{2+}_2\text{Me}^{3+}_2(\text{OH})_2[\text{PO}_4]_4]^{-}$  found in the crystal structure of jahnsite.

and  $\cos \beta' = (a^2/4 + c'^2 - 4c^2)/ac'$ . This provides a pseudo-orthogonal cell with dimensions  $a, b, c', \beta' \sim 90^\circ$ . It is observed that as  $\beta'$  approaches  $90^\circ$  for certain compositions, the frequency of twinning increases. These pseudo-orthogonal coordinates are  $a$  14.94 Å,  $c'$  18.65 Å, and  $\beta'$   $88^\circ 06'$  for the jahnsite used in this study.

A projection of the metals down  $[010]$  in Figure 4 shows why jahnsite twins. We observe a profound substructure, with subcell  $a(\text{sub}) = a/4$  and  $c(\text{sub}) = c'/2$  on the projection. Thus,  $h0l$  photographs of jahnsite can be easily mistaken as possessing an "orthogonal" cell. We observe, however, that when the heights in  $y$  are included (Fig. 4), the three-dimensional pseudo-orthogonality ceases to exist. We also note that  $a, b$ , and  $c'$  approximate segelerite

in dimension, which has  $a$  14.83 Å,  $b$  18.75 Å,  $c$  7.31 Å,  $Pcca$ . A preliminary structure analysis of segelerite shows that it *cannot* be continuously transformed into the jahnsite structure by mere distortions of the polyhedra. For this reason, jahnsite and segelerite represent two separate (but related) structure types, separated by the barrier of the relative locations of the  $[\text{PO}_4]$  tetrahedra.

#### Bond Distances

Table 4 provides a list of the individual polyhedral bond distances for jahnsite. The most extreme distortions are found for the  $\text{CaO}_6$  and  $\text{MnO}_6$  octahedra since they share edges with  $[\text{PO}_4]$  tetrahedra and with each other. We note that the short  $\text{O}(5)\text{-O}(7)$  distance, 2.442 Å, is the edge shared between

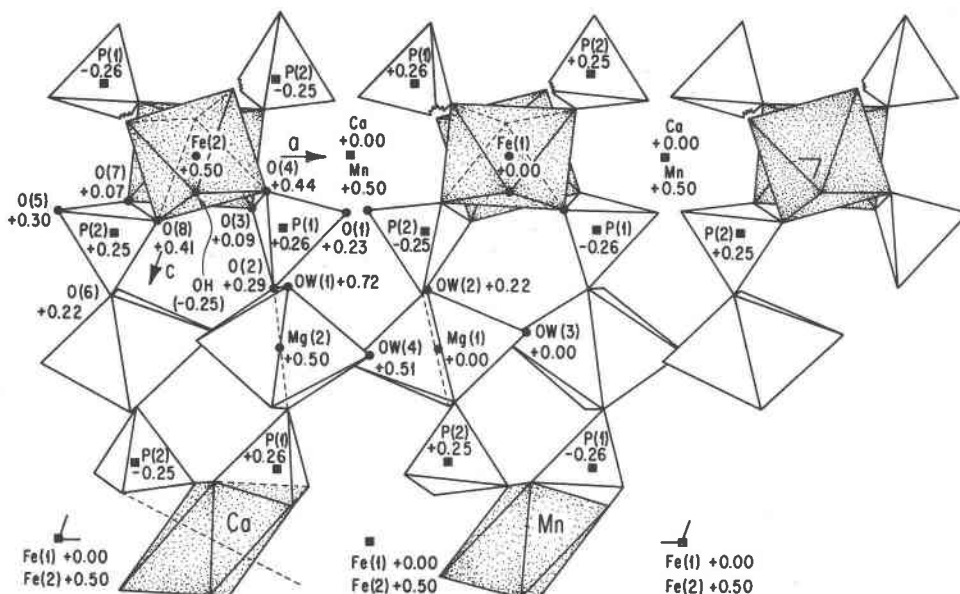


FIG. 3. Polyhedral diagram of the actual jahnsite structure. Some atoms have been left out to improve visualization. Heights are fractional coordinates in  $y$ .

CaO<sub>6</sub> and P(2)O<sub>4</sub>. It is also the shortest edge distance for that tetrahedron. Likewise, O(1)-O(4), which equals 2.422 Å, is the edge shared between MnO<sub>6</sub> and P(1)O<sub>4</sub> and is that tetrahedron's shortest edge as well. Finally, O(5)-O(5)'' 2.822 Å and O(1)-O(1)'' 2.830 Å are edges shared between CaO<sub>6</sub> and MnO<sub>6</sub> polyhedra and are next in rank of shortness for their polyhedra. All of these distortions are consistent with the repulsion of cations across shared edges. In addition, the CaO<sub>6</sub> octahedron is more distorted and considerably larger than the MnO<sub>6</sub> octahedron, providing evidence that these cations are ordered.

The remaining polyhedra do not share topological elements other than corners and, consequently, their range of distortion is less. The polyhedral averages in the abstract and in Table 4 are all consistent with grand averages found for these cations in such oxygen coordination. The Mg(O,H<sub>2</sub>O)<sub>6</sub> octahedra are substantially distorted. Since no elements other than corners are shared, these distortions result from deviations from local electrostatic neutrality and from hydrogen-bond formation.

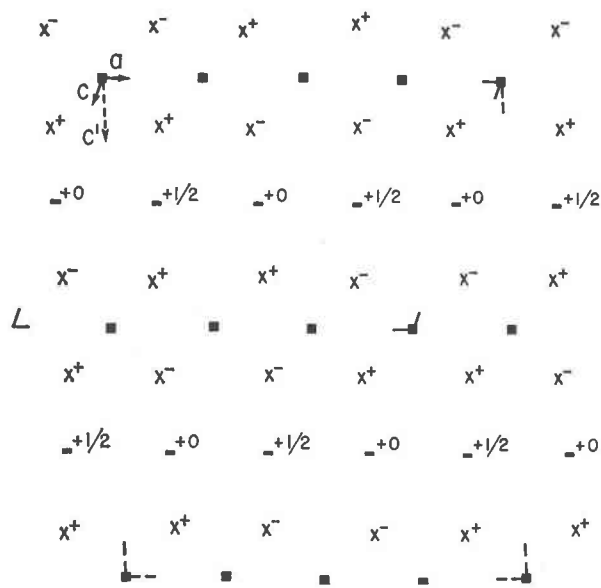


FIG. 4. Pseudo-orthogonal cell  $a \times c'$  found in jahnsite. The structure cell used in this study is also outlined. Interpretation of symbols: solid squares = Me<sup>2+</sup> and Me<sup>3+</sup> at  $y = 0, 1/2$ ; crosses are P atoms, and solid bars are Mg atoms.

TABLE 4. Jahnsite. Polyhedral Interatomic Distances†

Fe(1)		Ca		Mg(1)		P(1)	
2 Fe(1)-O(7)	1.966 Å	2 Ca -O(1)	2.331 Å	2 Mg(1) -O(6) <sup>ii</sup>	2.047 Å	1 P(1)-O(2)	1.510 Å
2 " -O(3)	1.973	2 " -O(5)	2.427	2 " -OW(2)	2.108	1 " -O(3)	1.539
2 " -OH	1.981	2 " -O(7)	2.497	2 " -OW(3)	2.108	1 " -O(1)	1.562
average	1.973	average	2.418	average	2.088	1 " -O(4)	1.562
						average	1.543
2 O(3) -O(7)	2.671	2 O(5) -O(7)	2.442**	2 OW(2) <sup>i</sup> -O(6) <sup>ii</sup>	2.774	1 O(1) -O(4)	2.422**
2 O(3) -OH	2.733	1 O(5) -O(5) <sup>ii</sup>	2.822*	2 OW(3) <sup>i</sup> -O(6) <sup>ii</sup>	2.924	1 O(1) -O(3)	2.494
2 O(7) -OH	2.787	1 O(1) -O(1) <sup>ii</sup>	2.830*	2 OW(3) -O(6) <sup>ii</sup>	2.953	1 O(2) -O(3)	2.503
2 OH -O(7) <sup>i</sup>	2.794	2 O(1) -O(7) <sup>ii</sup>	3.207	2 OW(2) -OW(3) <sup>i</sup>	2.970	1 O(1) -O(2)	2.552
2 OH -O(3) <sup>i</sup>	2.856	2 O(1) -O(5) <sup>ii</sup>	3.865	2 OW(2) -OW(3)	2.992	1 O(2) -O(4)	2.556
2 O(3) -O(7) <sup>i</sup>	2.894	2 O(1) -O(7) <sup>ii</sup>	3.933	2 OW(2) -O(6) <sup>ii</sup>	3.093	1 O(3) -O(4)	2.577
average	2.789	2 O(5) -O(7) <sup>ii</sup>	3.964	average	2.951	average	2.517
		average	3.373				
Fe(2)		Mn		Mg(2)		P(2)	
2 Fe(2) -O(8)	1.938	2 Mn -O(5)	2.116	2 Mg(2) -O(2)	2.033	1 P(2) -O(6)	1.508
2 " -O(4)	1.988	2 " -O(4)	2.215	2 " -OW(4)	2.083	1 " -O(8)	1.523
2 " -OH	1.993	2 " -O(1)	2.238	2 " -OW(1)	2.152	1 " -O(7)	1.548
average	1.973	average	2.190	average	2.089	1 " -O(5)	1.551
						average	1.533
2 OH -O(8) <sup>i</sup>	2.712	2 O(1) -O(4)	2.422**	2 O(2) -OW(4) <sup>ii</sup>	2.801	1 O(5) -O(7)	2.442**
2 O(4) -O(8) <sup>i</sup>	2.760	1 O(5) -O(5) <sup>ii</sup>	2.822*	1 O(2) -O(2) <sup>ii</sup>	2.884	1 O(6) -O(8)	2.490
2 O(4) -O(8)	2.791	1 O(1) -O(1) <sup>ii</sup>	2.830*	2 OW(1) -OW(4)	2.892	1 O(5) -O(6)	2.495
2 OH -O(4) <sup>i</sup>	2.799	2 O(4) -O(5)	3.105	1 OW(1) -OW(1) <sup>ii</sup>	2.910	1 O(5) -O(8)	2.512
2 OH -O(4) <sup>i</sup>	2.830	2 O(4) -O(5) <sup>ii</sup>	3.321	2 OW(1) -OW(4) <sup>ii</sup>	2.970	1 O(6) -O(7)	2.526
2 OH -O(8)	2.844	2 O(1) -O(5) <sup>ii</sup>	3.356	2 OW(1) -O(2)	3.032	1 O(7) -O(8)	2.544
average	2.789	2 O(1) -O(4) <sup>ii</sup>	3.446	2 O(2) -OW(4)	3.128	average	2.502
		average	3.079	average	2.953		

†Estimated standard errors: Me-O ± 0.006 Å, O-O' ± 0.009 Å.

\*Ca-Mn shared edges, \*\*Me<sup>2+</sup>-P shared edges.

<sup>i</sup> = -x, -y, -z; <sup>ii</sup> = 1/2-x, y, -z; <sup>iii</sup> = 1/2+x, -y, z applied to the coordinates in Table 2.



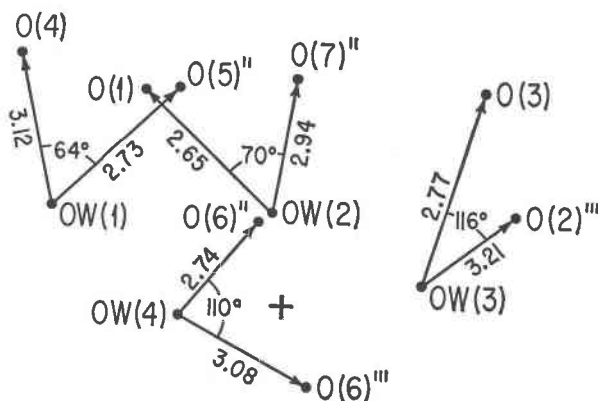


FIG. 5. Proposed hydrogen bonding scheme in one asymmetric unit for jahnsite down [010]. The cross is at  $x = 1/2$ ,  $z = 1/2$ .

### Hydrogen Bonds and Electrostatic Valence Balances

It was not possible to ascertain locations of the hydrogen atoms directly, but the geometrical restrictions are severe enough to warrant proposal of a hydrogen-bond model. The structure consists of the dense slabs  $[\text{CaMnFe}^{3+}_2(\text{OH})_2[\text{PO}_4]_4]^{4-}$  oriented parallel to  $\{001\}$  and weakly linked by the  $\text{Mg}(\text{O}, \text{H}_2\text{O})_6$  octahedra. Hydrogen bonds from OW(1), OW(2), OW(3), and OW(4) connect to the  $\text{O}_p$  oxygens in these slabs resulting in a herringbone pattern for these bonds. Distances and angles for the proposed model are featured as an asymmetric unit in Figure 5. They can be divided into short bonds OW(1) . . . O(5)'' 2.73 Å, OW(2) . . . O(1) 2.65, OW(3) . . . O(3) 2.77 Å, and OW(4) . . . O(6)'' 2.74; and long, more weakly linked bonds OW(1) . . . O(4) 3.12 Å, OW(2) . . . O(7)'' 2.94, OW(3) . . . O(2)''' 3.21 and OW(4) . . . O(6)''' 3.08 Å. Owing to its geometrical separa-

tion,  $(\text{OH})^-$  does not appear to form a strong bond since the only distances less than 3.0 Å are along polyhedral edges.

From this model, a tabulation of electrostatic balances of cations about anions is offered (Table 5). Hydrogen bond receptors are given  $\xi = +1/6$ , as suggested by Baur (1970). The resulting undersaturated anions, O(2) and O(8), reveal polyhedral distances shorter than average, and the oversaturated anions O(4) and O(7) show a tendency toward longer-than-average polyhedral bond distances. The remaining anions are sufficiently close to neutrality to show no such correlation with their polyhedral distances.

### Properties of the 7 Å Chain Structures

The resulting structures possess key features of benefit to the crystal chemist who is concerned with physical properties as well: the distance between slabs usually corresponds to the strongest low-angle intensities on powder and single crystal photographs and is, in addition, the plane of perfect cleavage. These relationships are also preserved in the "5 Å fiber axis" structures of basic ferrous-ferric phosphates, as noted by Moore (1970b) in a general review of the problem, although in these structures, the slabs are based on a different structural principle. A perplexing result for the mineralogist is an uncanny physical similarity among compounds within each structural group: the 7 Å structures involving  $\text{Fe}^{3+}\text{-O}$  octahedral chains are yellow to orange in color, and the 5 Å structures involving  $\text{Fe}^{3+}\text{-Fe}^{2+}\text{-Fe}^{3+}$  face-sharing trimers are all deep greenish-black and fibrous. We have found by experience that the most faithful means of distinguishing species within a group by visual means only is careful examination of their crystal morphology. To illustrate how frequent these structural principles are manifest in natural compounds, we note that among the phosphates laueite, gordonite, paravauxite, metavauxite, wavellite, pseudolaueite, childrenite, eosphorite, tavorite, strunzite, amblygonite, stewartite, jahnsite, overite, and segelerite are known to belong to the 7 Å chain structures; and dufrenite, rockbridgeite, laubmannite, "mineral A," beraunite, lipscombite, barbasalite, and souzalite are known to belong to the 5 Å fiber structures. This accounts for over 40 percent of the known basic  $\text{Me}^{3+}$  phosphate species! Since some of these species form under narrow conditions of  $T$ ,  $p\text{O}_2$  and  $\text{pH}$  and since practically no synthetic work has been done on these

TABLE 5. Jahnsite. Electrostatic Valence Balances of Cations about Anions†

Anions	Coordinating cations	Bond strengths	$\Delta\Sigma$
O(1)	P(1)+Mn+Ca+H(short)	5/4+2/6+2/6+1/6	+0.08
O(2)	P(1)+Mg(2)+H(short)	5/4+2/6+1/6	-0.17
O(3)	P(1)+Fe(1)+H(short)	5/4+3/6+1/6	-0.08
O(4)	P(1)+Fe(2)+Mn+H(Long)	5/4+3/6+2/6+1/6	+0.23
O(5)	P(2)+Mn+Ca+H(short)	5/4+2/6+2/6+1/6	+0.08
O(6)	P(2)+Mg(1)+H(short)+H(Long)	5/4+2/6+1/6+1/6	-0.08
O(7)	P(2)+Fe(1)+Ca+H(average)	5/4+3/6+2/6+1/6	+0.23
O(8)	P(2)+Fe(2)	5/4+3/6	-0.25
OH	Fe(1)+Fe(2)	3/6+3/6	0.00
OW(1)	Mg(2)-2H	2/6-2/6	0.00
OW(2)	Mg(1)-2H	2/6-2/6	0.00
OW(3)	Mg(1)-2H	2/6-2/6	0.00
OW(4)	Mg(2)-2H	2/6-2/6	0.00

†H(short) are bonds less than 2.8 Å, H(long) are bonds longer than 2.9 Å.  $\Delta\Sigma$  is the deviation from neutrality ( $\Sigma = 2.00$  for  $\text{O}^{2-}$ ; 1.00 for  $\text{OH}^-$  and 0.00 for  $\text{H}_2\text{O}$ ).

systems, the list of as yet unknown compounds belonging to this group is probably much larger.

### Acknowledgments

This study was possible through support from NSF GA 10932-A1 and the Sloan Foundation Grant-in-Aid BR-1489 awarded to P.B.M.

### References

- BAUR, W. H. (1969) A comparison of the crystal structures of pseudolaueite and laueite. *Am. Mineral.* **54**, 1312-1323.
- (1970) Bond length variation and distorted coordination polyhedra in inorganic crystals. *Trans. Am. Crystallogr. Assoc.* **6**, 129-155.
- BUSING, W. R., K. O. MARTIN, AND H. A. LEVY (1962) ORFLS, a Fortran crystallographic least-squares program. *U.S. Oak Ridge Nat. Lab. ORNL-TM-305*.
- CROMER, D. T., AND J. B. MANN (1968). X-ray scattering factors computed from numerical Hartree-Fock wavefunctions. *Acta Crystallogr.* **A24**, 321-324.
- JOHANSSON, G. (1962) On the crystal structures of  $\text{FeOHSO}_4$  and  $\text{InOHSO}_4$ . *Acta Chem. Scand.* **16**, 1234-1244.
- MOORE, P. B. (1970a). Structural hierarchies among minerals containing octahedrally coordinating oxygen: I. Stereoisomerism among corner-sharing octahedral and tetrahedral chains. *Neues Jahrb. Mineral. Monatsh.* **1970**, 163-173.
- (1970b) Crystal chemistry of the basic iron phosphates. *Am. Mineral.* **55**, 135-170.
- (1974) I. Jahnsite, segelerite, and robertsite, three new transition metal phosphate species. *Am. Mineral.* **59**, 48-59.
- RAMACHANDRAN, G. N., AND R. SRINIVASAN (1970) *Fourier Methods in Crystallography*. Wiley-Interscience, New York, p. 96-119.

*Manuscript received, February 22, 1974; accepted for publication, June 7, 1974.*